Available online at www.eccomasproceedia.org
Eccomas Proceedia COMPDYN (2023) 4095-4109

ECCOMAS
Proceedia

COMPDYN 2023
9th ECCOMAS Thematic Conference on
Computational Methods in Structural Dynamics and Earthquake Engineering
M. Papadrakakis, M. Fragiadakis (eds.)
Athens, Greece, 12-14 June 2023

FRAGILITY CURVES FOR BRIDGES SUBJECTED TO THREE-DIMENSIONAL SEISMIC ENVIRONMENTS

Jimena Rosas[1], Juan M. Mayoral[1*], and Mauricio Anaya[1]

[1] Institute of Engineering National University of Mexico, Mexico City, Mexico

*email: JMayoralV@iingen.unam.mx

Abstract

Bridges built on soft soils, such as highly compressible plastic clays, may present a greater seismic vulnerability due to the low shear strength, high compressibility, low stiffness, small damping increment with shear strain, and high plasticity index, which can lead to large amplifications of the seismic movements. These factors entail a greater probability of experiencing failures in the foundation or structure, which result in the loss of functionality and interruption of the transport network. Therefore, the design of urban bridges built on soft soils and located in densely populated cities requires using numerical models to establish the probability of reaching or exceeding a given damaged state in a seismic event. This paper presents a vulnerability assessment of an urban bridge built on the typical soft soils found in Mexico City. *The evaluations were carried out considering both normal and subduction fault events expressed in uniform hazard spectra for several return periods (i.e., 125, 187.5, 250, 362.5, 475, 1475, and 2475 years), assuming a three-dimensional seismic environment. Site response analyses and site-specific numerically derived fragility curves were used to assess the critical supports probability of reaching or exceeding a given damage state. The system's seismic response was characterized using a series of three-dimensional numerical models developed with the software FLAC3D. The effect of both soil conditions and ground motion characteristics on the soil-structure system response was accounted for in the analyses. The damage index was defined in terms of earthquake-induced transversal, longitudinal, and vertical upper deck displacements associated with column cracking and potential loss of support of the upper deck beam. The vulnerability of the analyzed bridge was established.*

Keywords:
Damage in bridges
Soil-structure interaction
Fragility curves
Damage index

ISSN:2623-3347
Peer-review under responsibility of the organizing committee of COMPDYN 2023.
doi: 10.7712/120123.10704.20541

1 INTRODUCTION

The failures of bridges and urban overpasses during earthquakes [1-10] have demonstrated the importance of defining an adequate approach to evaluate and improve the performance of these systems against extreme events.

Fragility curves have been developed using two-dimensional seismic environments with frequency domain analysis [11,12], without considering the effect of vertical ground motion on the seismic response of the system. Limited studies have developed dynamic analyzes for bridges integrating the vertical ground motions without considering the effect of soil-foundation-structure interaction, site effects and frequency content [13-16]. In this regard, it has been seen that the use of three-dimensional seismic environments realistically considers the behavior of the structures. In addition, taking into account the vertical component of movement implies inducing changes in the magnitude of the axial load of structural elements, which is a factor that determines their capacity [17, 18].

For seismic design, the vertical component acceleration has been considered as a fraction of the magnitude of horizontal movement. Rosenblueth (1975) [19] identified that the relationship between the vertical and horizontal components is not constant and depends on the structure period. Newmark (1979) [20] determines that the vertical component should be estimated as 2/3 of the peak value of the horizontal component of movement. In turn, Bozorgnia (1995) [21] observed that the main characteristic of the Loma Prieta (1989) and Taiwan (1999) earthquakes was the V/H relationship since it was notably exceeded with a value much higher than 2/3, so it is shown that the relationship between the vertical and horizontal movement V/H depends on the distance to the place where the earthquake originated.

Currently, there are no seismic fragility curves for bridges that consider the three-dimensional seismic environment and soil-foundation-structure interaction in soft soils like those found in Mexico City. The fragility curves derived from this research work will be based on the PGA, which will be applied in the evaluation of bridges located on soft soils.

2 METHODOLOGY

The proposed methodology (figure 1) consists of five main stages: 1) selection of the site study, 2) characterization of the seismic environment in terms of uniform hazard spectra, UHS. In our case study, synthetic acceleration time histories were developed for normal and subduction events considering seven return periods, 3) identification of failure modes and damage intervals for the most common types of bridges built on soft soils. For this case study, the damage index was considered in terms of longitudinal, transversal, and vertical displacements of the pier induced by the earthquake, which are associated with column cracking and loss of support of the upper deck of the bridge, 4) generation of three-dimensional numerical models of finite differences to simulate and evaluate the effects of the soil-foundation-structure seismic interaction and, 5) generation of fragility curves to assess the probability that the critical supports reach or exceed a given damage state, through a parametric study for different return periods.

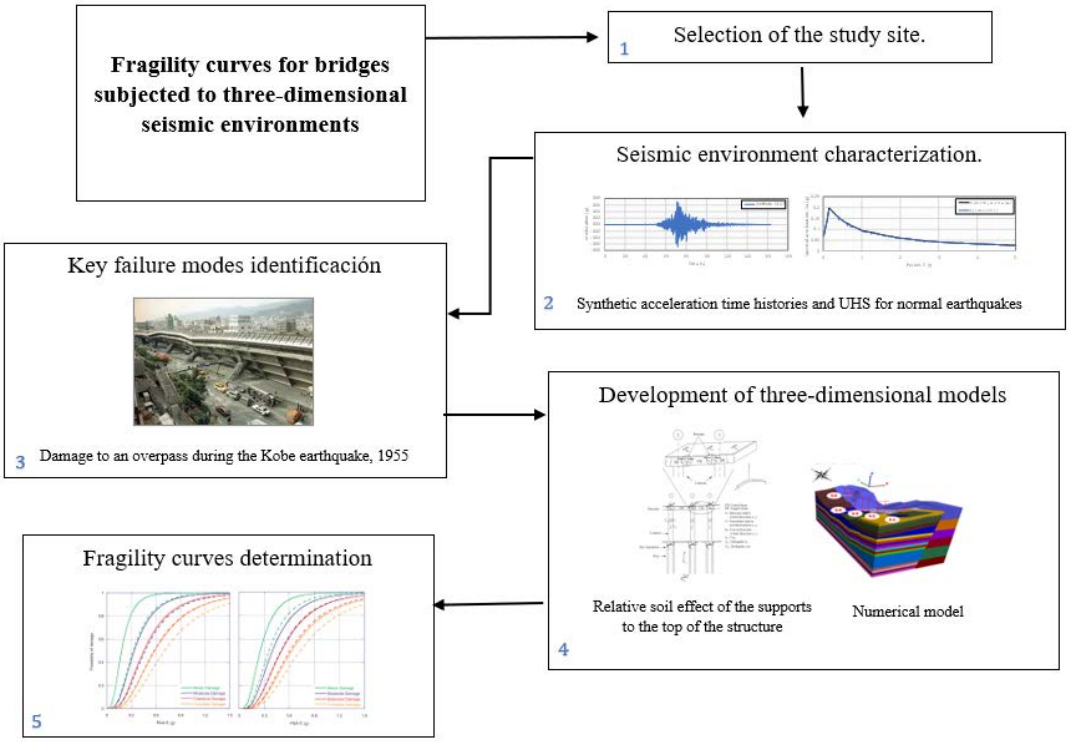

Figure 1: Proposed methodology to develop fragility curves for bridges. (Modified from [11]).

2.1 Derivation of fragility curves

Fragility curves were developed for the longitudinal, transversal, and vertical directions using a typical bridge typology of Mexico City. The different ground motions depend on amplitude, frequency content, and duration. The damage level was estimated in terms of the maximum lateral displacement of the column normalized by its average height, and it is related to the peak ground acceleration in the free field, PGA_{ff}. Equation 1 calculates the probability of reaching or exceeding different damage states for a ground motion level. Each fragility curve is characterized by a mean value of soil movement and an associated dispersion factor (lognormal standard deviation). Ground motion is estimated in terms of the peak ground acceleration, PGA, or spectral acceleration, S_a, and ground failure is quantified in terms of permanent ground deformations, PGD [22].

$$P_f\left(ds \geq ds_i \middle| PGA_{ff}\right) = \emptyset\left[\frac{1}{\beta_{tot}} In\left(\frac{PGA_{ff}}{PGA_{ffmi}}\right)\right] \quad (1)$$

where $P_f(\cdot)$ denotes the probability of reaching or exceeding a particular damage state, *ds*, for a given seismic intensity level defined by the seismic intensity measure (i.e., PGA_{ff}), Φ is the standard cumulative distribution, PGA_{ffmi} is the median threshold value of the earthquake intensity measurement required to cause the i-th damage, and β_{tot} is the total logarithmic standard deviation.

This last parameter is estimated from the following expression $\beta_{tot} = \sqrt{\beta ds^2 + \beta C^2 + \beta D^2}$, where β_{tot} includes three sources of uncertainty: the definition of damage states (βds), the response and resistance (capacity) of the element (βC), and the variability in the earthquake input motion (demand) (βD).

Following the HAZUS [23] approach, βds is set equal to 0.4, βC is considered equivalent to 0.4 as presented by Franchetti et al. [4], and βC is calculated based on the variability of the different ground motions. The median threshold value of the seismic parameter, mi, is obtained

for each damage state as a function of the evolution of the damage with the increase in the earthquake's intensity.

Based on the criteria shown by Franchetti [4] and considering the damage states proposed by Jin-Hak [24], five different damage states were established. These damage states are none, ds1, slight/minor, ds2, moderate, ds3, extensive, ds4, and complete, ds5.

2.2 Damage index and damage states

Slight bridge damage, ds2, is identified by the appearance of minor cracks and detachments in the abutment, cracks in the abutment key, little detachments in the hinges, a minor detachment in the column, or by minor cracking in the spine. Moderate damage, ds3, is defined by any column that shows shear cracks, moderate movements in the abutment (<2"), connections that have broken shear keys or bent bolts, bearing failure, etc. Extensive damage, ds4, is seen for any column that degrades short of collapse (shear or flexural failure), significant residual movement at connections, vertical displacement at the abutment, differential column displacements, and settlements. Complete damage, ds5, is defined by any column that collapses and the connection loses all bearing support, which can lead to the imminent collapse of the deck or tilting of the sub-structure due to foundation failure.

3 CASE STUDY

The case study was located in the soft soil of Mexico City, where it is common to find highly compressible plastic clays. The typology of this overpass is similar to the Viaducto Bicentenario and the North and South Urban Highways of Mexico City [25]. These bridges are single-deck prestressed concrete precast structures with bearing surfaces ranging from 2 to 6 lanes.

The overpass typology comprises hollow central beams with a trapezoidal section 40 m long, precast in high-resistance prestressed concrete, and on which lies a 9 m wide platform of the same material. Above the platform, a structural firm forms a rigid diaphragm and increases the resistance of the same platform, and the asphalt layer acts as a rolling surface (figure 6a).

In the same way, the 12 m high column has a hollow rectangular section, it is a precast element of high-resistance prestressed concrete. The union of the column and the bridge platform is connected with a head made of the same material as that of the column. In this way, all the elements are structurally attached.

The support foundation is made up of a compensated reinforced concrete square box placed (width 12.5 m) at a depth of 6 m. The cushion slab's top, bottom, and walls are 40 cm thick (figure 3). Below the foundation box are nine reinforced concrete piles, each 9 m long and with a square cross-section of 0.50 m on each side. Therefore, the total depth of the foundation is 15 m, contemplating the foundation box and the piles as shown in figure 6a. In this type of foundation, it is sought that the piles mitigate the settlements [26-28] improve the seismic design [29-31], and mitigate problems related to subsidence [32]. Both lie the offset box will distribute the load capacity of the substructure.

3.1 Soil profile

The bridge studied is located in the Lake Zone of Mexico City [33]. The study site was analyzed by Mayoral and Mosqueda [34].

Figure 2 shows the stratigraphic profile and the shear wave velocity distribution of the analyzed site. Typically, the stratigraphic profile in this area exhibits a desiccated clay crust on top, extending to a depth of 5.0 m, which is underlain by a layer of soft clay approximately 30.0 m thick, with interbedded lenses of sandy silts and silty sands. Beneath the clay is a layer 5.0 m thick, on average, of very dense sandy silt, which rests on a layer of rigid clay that descends to a depth of 40.0 m. Below this elevation is found a competent layer of very dense sandy silt.

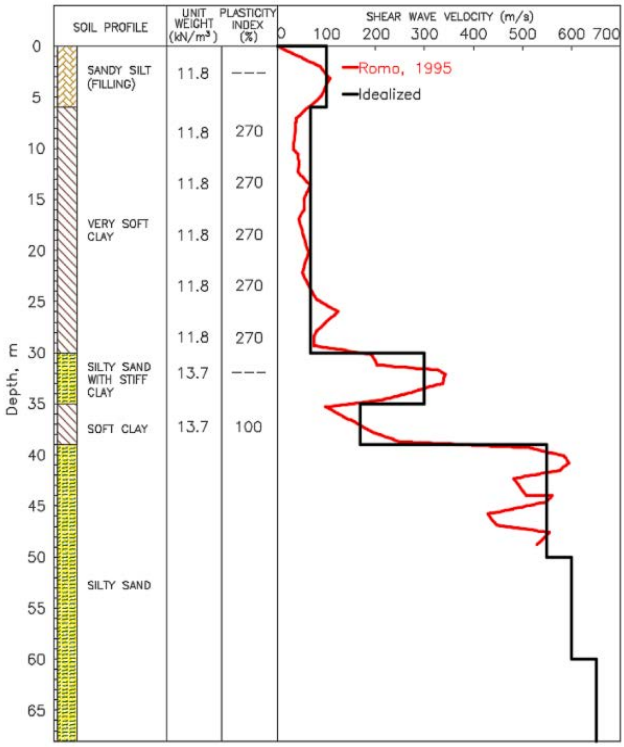

Figure 2: Soil profile and shear wave velocity distribution of the analyzed site.

Normalized modulus degradation and damping curves for sands were estimated by Seed and Idriss [35]. To characterize the degradation of the stiffness and the increase in damping of the clays during the seismic event, the Gonzalez and Romo [36] model was used, see figure 3. The shear wave velocity distribution was obtained by Seed et al. [37] using the down-hole and P-S suspension logging techniques and is also included in figure 3.

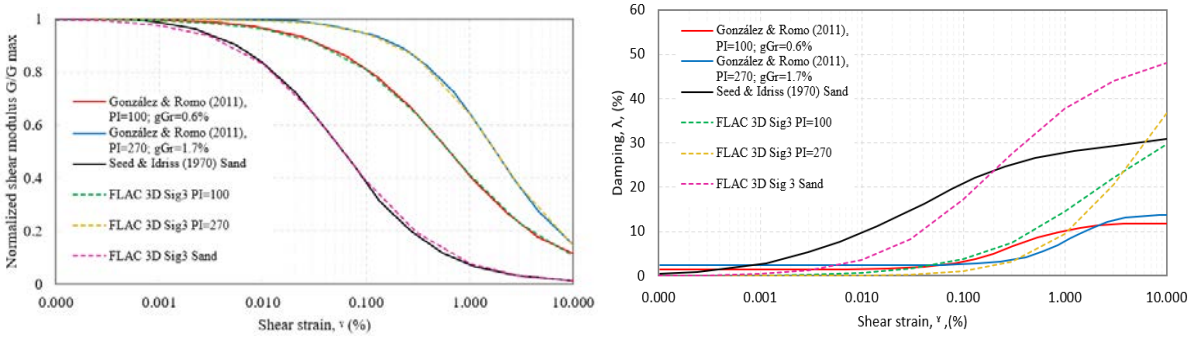

(a) (b)

Figure 3. Normalized (a) shear stiffness degradation, G/G_{max}, and (b) damping λ curves.

3.2 Seismic environment

The seismic hazard of Mexico City is controlled by interplate earthquakes along the subduction zone on the Pacific coast, such as the September 19, 1985 earthquake; as well as intra-plate earthquakes in the subducted Cocos plate [5, 32].

The seismic environment was established through uniform hazard spectra developed for seven return periods considering normal and subduction events. The soil-foundation-bridge seismic interaction was analyzed with six ground motions, as shown in Table 1.

Seismo-genic Zone	Earthquake name	Location	Year	Moment magnitude [Mw]	Epicentral distance, Ed [km]	PGA [g]	Duration [s]
Normal	Umbria	Umbria Marche, Italy	1998	4.8	10	0.223	40
	Montenegro	Montenegro, Yugoslavia	1979	6.9	21	0.251	48
	CU17	Puebla, Mexico	2017	7.1	122	0.059	281
Subduc-tion	CU85	Michoacan, Mexico	1985	8.1	419	0.033	73
	Chile	Maule, Chile	2010	8.8	109	0.638	120
	Japan	Honshu, Japan	2011	9	283	0.939	300

Table 1: Ground motions used in the analysis.

Synthetic ground motions were developed so that their 5% damped response spectrum reasonably matches the design response spectrum, using the method proposed by Lysmer [38], and modified by Abrahamson [39]. In this way, the signals induced in the three-dimensional model of the bridge represent a realistic design condition for the site.

According to Newmark [20], horizontal accelerations were considered complete, and 60 and 30% were in the vertical component of movement for normal and subduction earthquakes, respectively.

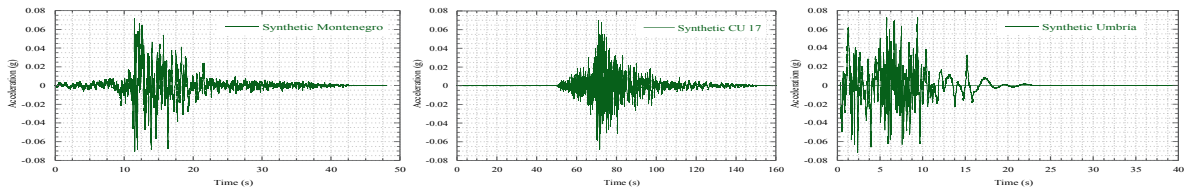

(a)

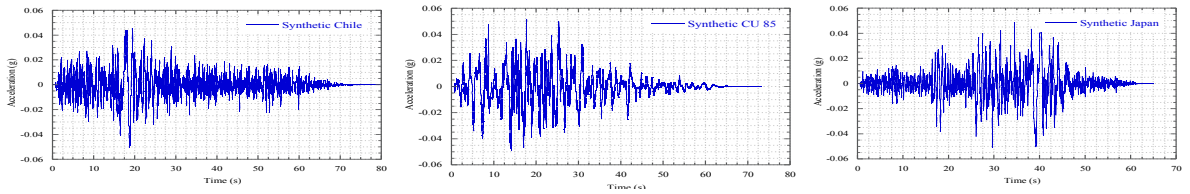

(b)

Figure 4: Synthetic time histories, for (a) normal, and (b) subduction events for a return period of 250 years.

The adjusted synthetic acceleration time histories for the normal and subduction earthquakes for TR=250 years are shown, respectively, in figure 4. The acceleration time histories were adjusted for each earthquake event and each return period (125, 187.5, 362.5, 475, 1475, and 2475 years) considered in the analysis (figure 5).

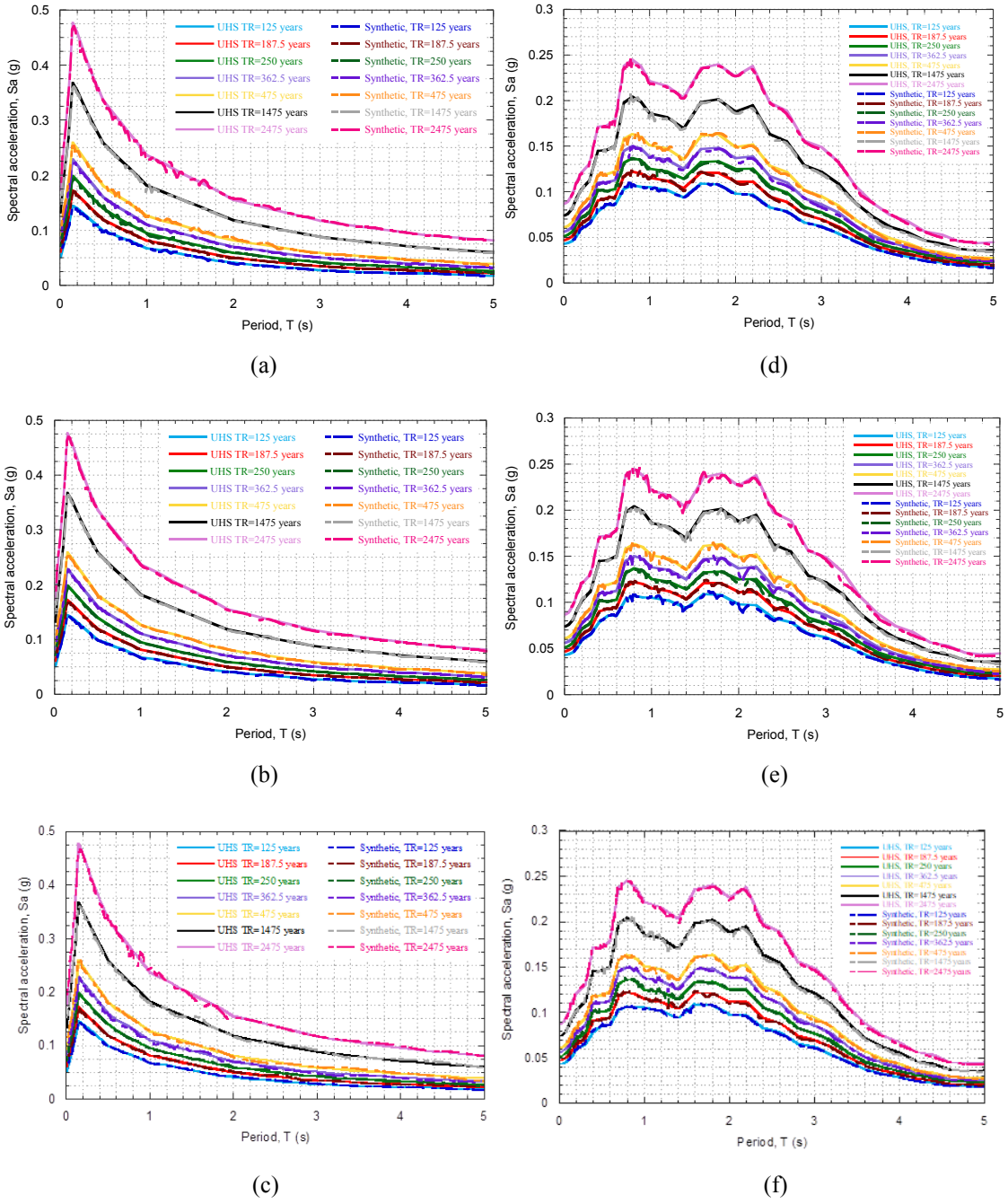

Figure 5: Uniform hazard spectra and adjusted ground motion response spectra for normal and subduction events: (a) CU 17, (b) Montenegro, (c) Umbria, (d) Chile, (e) CU 85 y (f) Japan.

3.3 Numerical model

To evaluate the seismic response of the system, a series of three-dimensional finite difference numerical models were developed using the FLAC3D software [40] considering the non-linearity of the soil in clayey materials.

A non-linear elastic behavior model was used, which tries to characterize the transient ground response in each load cycle as a function of the evolution of shear strains during ground shaking, rather than the steady state response established in the resonant column and cyclic triaxial test, from which modulus degradation and damping curves (figure 3). The free field

boundaries implemented in FLAC3D were used along the edges of the model, to avoid energy reflexing at the model edges, and represent free field conditions.

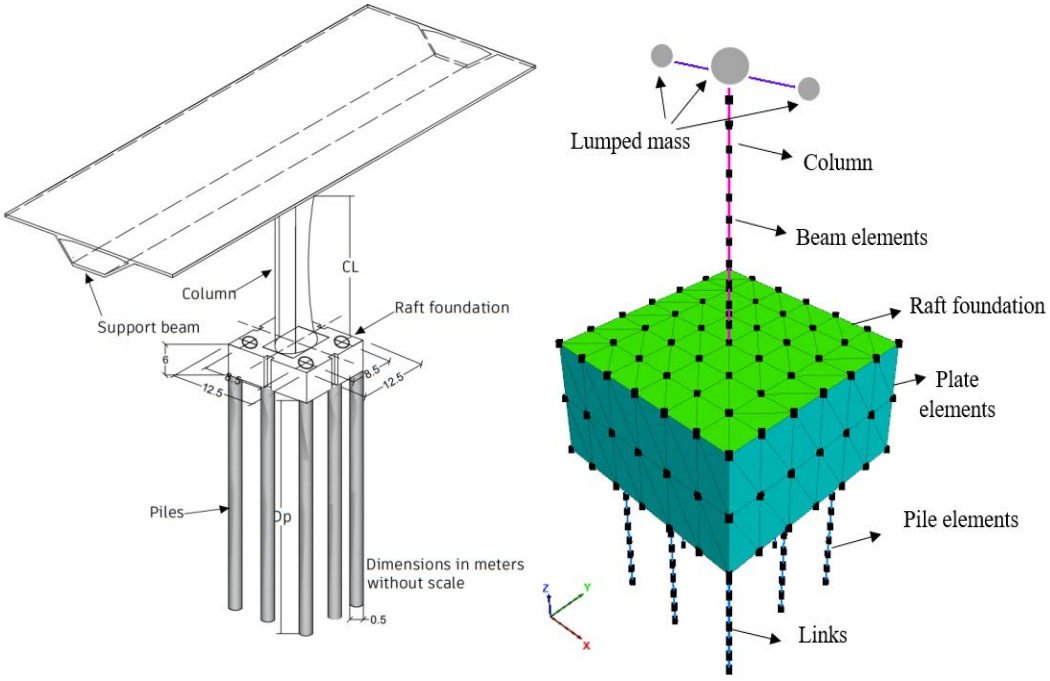

Figure 6: Schematic representation of (a) urban overpass y (b) three-dimensional model of finite differences.

The soil-structure system was divided into three stages: soil, foundation, and structure. The structure was modeled with three-dimensional beam elements and lumped masses, a foundation with plate elements, and piles with three-dimensional pile elements, which take into account the effects of diameter and the interaction between the pile and the surrounding soil (figure 6b).

3.4 Site response analyses

Initially, the free field condition was established from the results obtained from the one-dimensional analysis using the SHAKE software [41].

The free field boundaries implemented in FLAC^{3D} were used along the edges of the model, and a flexible base was considered at the bottom.

To consider the variation of the modulus stiffness degradation with the shear strain during the seismic event, the "Sig3" hysteretic model available in FLAC^{3D} [38] was used. The free field finite difference model is shown in figure 7. This model considers an ideal soil, in which the stress depends only on the deformation and not on the number of cycles. So, an incremental constitutive relationship of the degradation curve can be described by $\tau_n/\gamma = G/G_{max}$, where τ_n is the normalized shear stress, γ is the shear strain, and G/G_{max} the normalized secant modulus. The Sig3 model is defined by equation 2.

$$\frac{G}{G_{max}} = \frac{a}{1+\exp\left(-\frac{L-x_0}{b}\right)} \tag{2}$$

where L is the logarithmic deformation defined as L = log10 (g), and the parameters a, b and x_0, used by the Sig3 model, were obtained through an iterative approach, in which the modulus degradation curves were fitted with the model equations. The corresponding damping is given directly by the hysteresis loop during cyclic loading. For the cases studied herein, the parameters "a", "b" and "x_0" vary from 1 to 1.0035, -0.428 to -0.0559 and, 0.250 to -1.222, respectively.

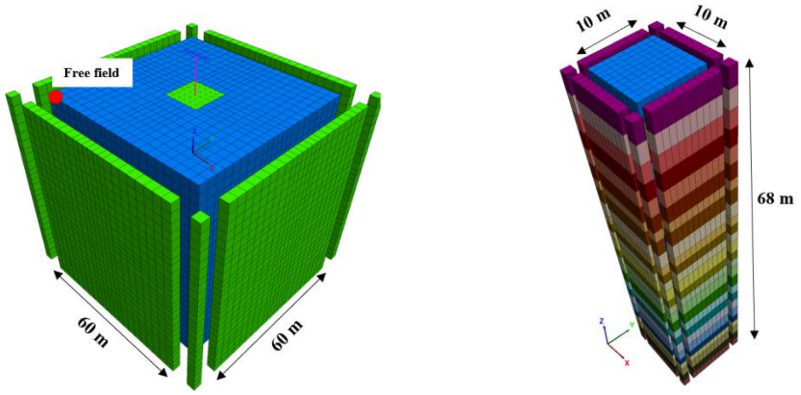

(a) (b)

Figure 7: Three-dimensional finite difference model, and soil column finite difference model.

Numerical distortion of the propagating wave can occur in a dynamic analysis depending on the modeling conditions. Both the input wave's frequency content and the system's wave velocity characteristics will affect the wave transmission's numerical precision. These lateral limits should be placed at sufficient distances to minimize propagating wave distortion and achieve free field conditions. For this case, the recommendation of Kuhlemeyer and Lysmer (1973) [38] was considered, where for an accurate representation of the transmission of waves through a model, the size of the spatial element, Δl, should be smaller. to one-fifth of the wavelength associated with the highest frequency component of the input wave containing appearing energy, fmax (for example, $\Delta l \leqslant \lambda/5$). In this case, the smallest average shear wave velocity Vs of the studied site in the soft clays ranges between 70 and 100 m/s, as shown in figure 3 and the highest significant frequency of excitation where the energy is concentrated is around 4.6 Hz. Therefore, the wavelength varies between 15 and 21 m, so it is appropriate to consider an Δl of 3 m. Models developed by Mayoral (2015) [42] have shown good agreement between finite difference models developed with FLAC3D and SHAKE for low to moderate levels of movement, using meshes with similar element sizes.

3.5 Soil-foundation-structure seismic interaction

The connection between the foundation box and the piles was considered embedded, although in practice the union of these two elements is at a joint, as can be seen in figure 6b. Said connection is designed to transmit loads axially to the pile and avoid perforation of the bottom slab. The characteristics of the elements for modeling the bridge are presented in Table 2.

Element	Model	Young's modulus (GPa)	Poisson ratio	Unit weight (kN/m^3)
Bridge superstructure	Beam elements	31.82	0.30	24
Square box	Plate elements	22.14	0.20	24
Piles	Pile elements	24.25	0.20	24

Table 2: Properties of the structural model.

For the dynamic analysis, the synthetic ground motions were applied in three directions x, y, and z (longitudinal, transversal, and vertical), considering 100% of the movement in the horizontal components and 60% and 30% in the vertical direction for normal earthquakes and subduction earthquakes, respectively.

For this case study, the damage index, DI see table 3, was established based on the lateral displacement of the column normalized by an average column height (i.e., 12 m), and in turn, in table 4, damage indices are shown for a two-dimensional seismic event [11].

Damage state (dsi)	ds1. None	ds2.Minor/ Slight	ds2. Moderate	ds4. Extensive	ds5. Complete
Range of damage index	DI ≤ 0.007	0.007< DI ≤ 0.015	0.015< DI ≤ 0.025	0.025< DI ≤ 0.050	DI> 0.050

Table 3: Damage state estimation for the urban overpass

Damage state (dsi)	ds1. None	ds2.Minor/ Slight	ds2. Moderate	ds4. Extensive	ds5. Complete
Range of damage index	DI ≤ 0.0025	0.0025< DI ≤ 0.0035	0.0035< DI ≤ 0.0045	0.0045< DI ≤ 0.006	DI> 0.006

Table 4: Damage state estimation for the urban overpass [11]

Figures 8 and 9 show the evolution of DI concerning the peak ground acceleration in free field, PGA_{ff}, in the transverse and longitudinal directions, along with an average exponential regression that fits the data set. Meanwhile, figure 10 show the fragility curves for normal and subduction earthquakes in both directions (transversal and longitudinal).

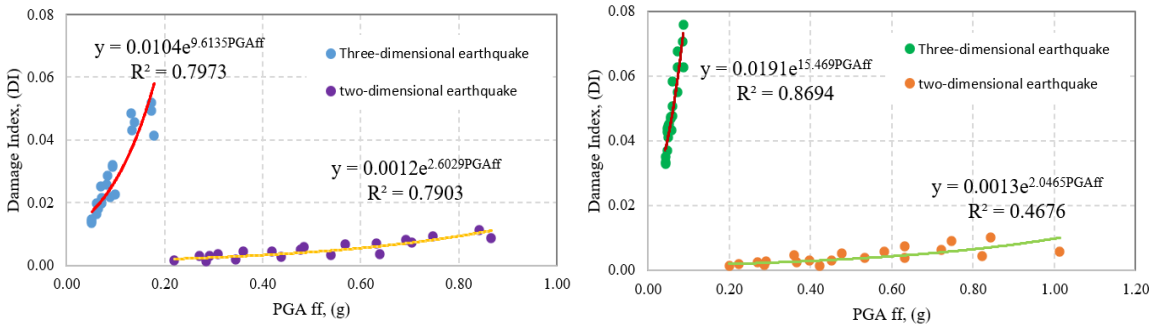

(a) (b)

Figure 8: Evolution of the DI (a) normal earthquakes (b) subduction earthquakes (Transversal direction).

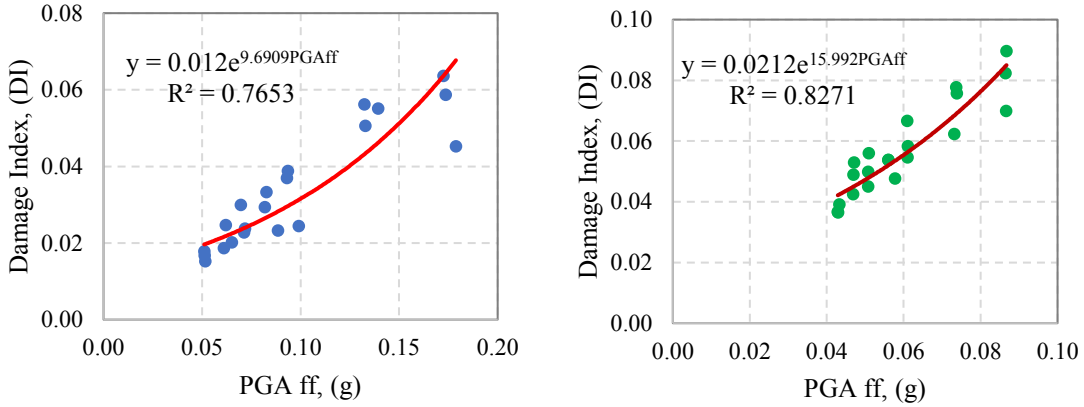

(a) (b)

Figure 9: Evolution of the DI (a) normal earthquakes (b) subduction earthquakes (longitudinal direction).

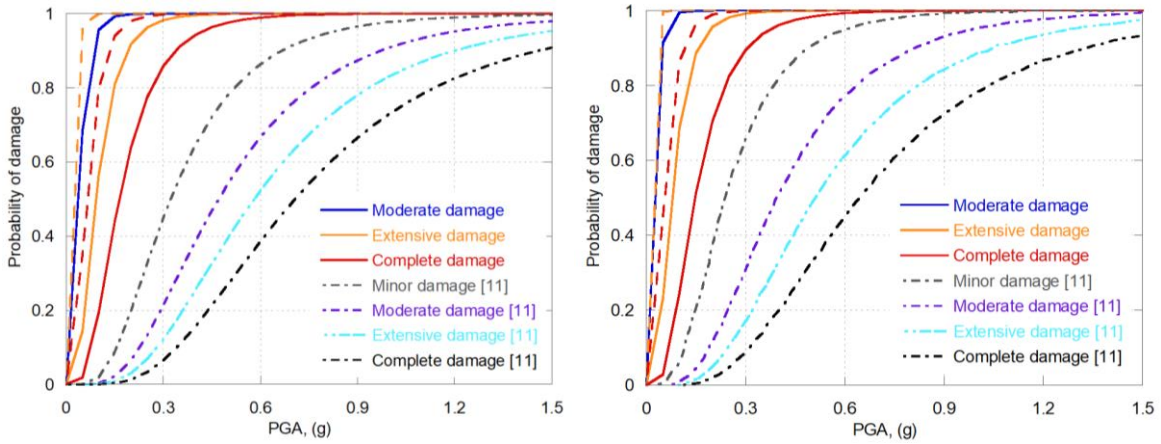

(a) (b)

Figure 10: Fragility curves for normal (solid lines) and subduction (dashed lines) events for (a) transversal and (b) longitudinal direction.

The fragility curves generated were compared with those obtained by Mayoral et al., [11], which were developed in rigid soils and with two-dimensional seismic environments. It can be observed that the probability of reaching a damage state is higher considering a three-dimensional seismic environment. Likewise, the probability of reaching a damage state increases due to the properties of soft soils that induce increased displacements of the structure, partially caused by the rocking effect. Therefore, the fragility curves are presented starting from a moderate damage state for normal and subduction earthquakes, respectively.

Comparing the two fragility curves, it can be seen that the greatest damage occurred in the bridge transversal direction (figure 11a). Complete damage is achieved with a PGA greater than 0.25 g for subduction earthquakes (dashed line) and 0.50 g for normal earthquakes (solid line).

Complete damage state was achieved first for subduction earthquakes due to most of the energy is concentrated in periods around 1 and 2 s, leading to large amplifications and lengthening of the duration of ground movements [33, 43] caused by high plasticity clay deposits. Likewise, a modification of the frequency content is produced, which in turn leads to a resonance effect, between the movements of the ground and the structure, as occurred during the Mw 8.1 09/19/1985 subduction fault earthquake, where the predominant period of the soil was found between 0.9 and 1.2 s, which coincides with the period of the structure (1.01 s), resulting

in a resonance effect. This was also accentuated due to the concentration of energy in the high frequency range (low period range of 0.15–1.0 s) [44].

Currently, the construction regulations for Mexico City consider a return period of 250 years. This implies that the index damage for this return period is extensive for both normal and subduction earthquakes. On the other hand, major return periods (362.5, 475, 1475, and 2475 years) present a complete damage state for normal and subduction events.

4 CONCLUSIONS

Fragility curves were generated for urban bridges located in densely populated urban areas, through a series of three-dimensional numerical models considering the site response, soil-foundation-structure interaction effects, and frequency content. It was observed that the probability of reaching a damage state is greater with the use of a three-dimensional seismic environment, because vertical movement increases the level of response and the amount of damage on a bridge. According to the site-specific fragility curves developed in this article, and the results obtained from the probabilistic analysis of site response, as well as the probability of reaching or exceeding a given damage state of the urban overpass, it can be noted that the highest probability of failure is reached with subduction events. Likewise, the probability of reaching a damage state increases due to the properties of soft soils that induce increased displacements of the structure, partially caused by the rocking effect.

REFERENCES

[1] M. Torres y M. Rodríguez, Capacidad de desplazamiento lateral de columnas para puentes de concreto reforzado y presforzado en zonas sísmicas. *XIX Congreso Nacional de Ingeniería Sísmica*, Veracruz, México, 2013.

[2] J. Bray y D. Frost, *Geo-engineering reconnaissance of the 2010 Maule, Chile earthquake*. Report of the NSF sponsored GEER association team No. GEER-022, 2010.

[3] D. Rivera y R. Meli, Procedimiento de diseño sísmico de columnas de puentes urbanos de concreto reforzado, *Revista de Ingeniería Sísmica*, nº 79, pp. 1-23, 2008.

[4] P. Franchetti, M. Grendence, C. Modena, D. Slejko y F. Bergo, Evaluation of seismic risk: application to bridges and viaducts in veneto (Italy), 13th *World Conference on Earthquake Engineering*. Vancouver, B. C., Canada. August, nº 2791, pp. 1-6, 2004.

[5] J. M. Pestana, R. B. Sancio, J. D. Bray, M. P. Romo, M. J. Mendoza, R. E. S. Moss, J. M. Mayoral Villa y R. B. Seed, Geotechnical engineering aspects of the June 1999 Central México earthquakes, *Journal Earthquake SPECTRA*, vol. 18, nº 3, pp. 481-499, 2002.

[6] R. Zelinski, *Post Earthquake Investigation Team Report for the Loma Prieta Earthquake*. California Department of Transportation. Division of Structures, Sacramento, Sacramento, 1994.

[7] M. Yashinsky, R. Oviedo, S. Ashford, L. Fargier-Gabaldon y M. Hube, *Performance of highway and railway structures during the February 27, 2010 Maule, Chile earthquake,* Maule, Chile, 2010.

[8] G. Housner, Competing against time. Report to Governor George Deukmejian from the Governor's Board of Inquiry on the 1989 Loma Prieta Earthquake. *Office of Planning and Research*, State of California, Mayo, p. 264, 1990.

[9] K. Kawashima , Damage of bridges resulting from fault rupture in the 1999 Kocaeli and duzce, Turkey earthquakes and the 1999 Chi-Chi, Taiwan earthquake*, Proceedings of Seismic Fault-induced Failures*, Tokyo, 2001, pp. 171-190.

[10] M. J. Priestley y Y. Uang, *Damage Analysis of Selected Freeway Bridges*, University of California, San Diego, Structural Systems Research, vol. 06, nº SSRP-94, 1994.

[11] J. M. Mayoral Villa, A. Badillo y J. M. Alcaráz Barranco, Vulnerability and recovery time evaluation of an enhanced urban overpass foundation, *Journal of Soil Dynamics and Earthquake Engineering,* vol. 100, nº ISSN 0267-7261, pp. 1-15, 2017.

[12] C. Gomez Soberon y I. Soria Rodriguez, Curvas de fragilidad para tres puentes carreteros típicos de concreto., Universidad Autonoma Metropolitana Azcapotzalco, Mexico., vol. 4, nº 2, pp. 15-11, 2013.

[13] A. J. Papazoglu y A. S. Elnashai, Analytical and field evidence of the damaging effect of vertical earthquake ground motion., *Journal Earthquake Eng Struct Dyn*, vol. 25, nº 10, pp. 1109-37, 1996.

[14] M. A. Saadeghvariri y D. A. Foutch, Dynamic behavior of R/C highway bridges under the combined effect of vertical and horizontal earthquake motions, Journal Earthquake Eng Struc Dyn , vol. 20, nº 6, pp. 535-49, 1991.

[15] C. P. Yu, Effect of vertical earthquake components on bridge responses., Ph. D. thesis, University of Texas at Austin, Austin., 1996.

[16] M. R. Button , C. J. Cronin y R. L. Mayes, Effect of vertical motions on seismic response of bridges., Journal Struct Eng, vol. 128, nº 12, pp. 1551-64, 2002.

[17] S. J. Jong, S. Abdollah, H. L. Do, C. Eunsoo y D. Reginald, Damage Assessment of older highway bridges subjected to three-dimensional ground motions: Characterization of shear-axial force interaction on seismic fragilities, Engineering Structures, vol. 87, pp. 47-57, 2015.

[18] E. Erduran y A. Yakut, Drift based damage functions for reinforced concrete columns, Computers & Structures, vol. 82, pp. 121-130, 2004.

[19] E. Rosenblueth y H. Contreras, Approximate design for multicomponent earthquakes, ASCE Journal of Engineering Mechanics, vol. 103, pp. 895- 911.

[20] N. M. Newmark y W. J. Hall, Earthquake spectra and design, Earthquake Engineering Research Institute, Berkeley, California, 1982.

[21] Y. Bozorgnia y N. Mansour, Characteristics of Free Field Vertical Ground Motion During the Northridge Earthquake, Earthquake Spectra, vol. 11, nº 4, pp. 515-525, 1995.

[22] K. Pitilakis, H. Crowley y A. M. Kaynia, SYNER-G:Typology Definition and Fragility Functions for Physical Elements at Seismic Risk, Springer.

[23] M. H. Hazus, Technical manuals, Washington, DC., 2004.

[24] Y. Jin-Hak, K. Sang-Hoon y K. Shigeru, PDF interpolation technique for seismic fragility analysis of bridges, Engineering Structures, vol. 29, pp. 1312-1322, 2007.

[25] M. J. Mendoza Lopez, E. Ibarra Razo, M. P. Romo Organista, M. Rufiar Jarquin, J. M. Mayoral Villa, W. P. Paniagua Zavala y E. Garces Camara, Pruebas de carga axial a compresión y extracción en pilas de cimentación instrumentadas del Viaducto Bicentenario, Estado de México, de XXV Raunion Nacional de Mecanica de suelos e ingenieria geotecnica., Acapulco,Guerrero, Mexico, 2010.

[26] M. J. Mendoza y G. Auvinet, The Mexico earthquake of September 19, 1985- behavior of biulding foundations in Mexico City, Journal, Earthq Spectra, vol. 4, nº 4, pp. 53-835, 1998.

[27] G. Auvinet, Seismic response of subsoil and building foundations in Mexico City (1985-2017), ISSMGE Touring Lecture, 2018.

[28] N. Riordan, A. Canavate, S. Kumar y F. Ciruela, Analysis of Friction Piles in Consolidating Soil., de NUMGE 2018 9th. European Conference on Numerical Methods in Geotechnical Engineering, 2018.

[29] M. Mendoza, Comportamiento de una cimentacion con pilotes de friccion, Ciudad de Mexico: Programa de maestria y doctorado en ingenieria, UNAM, 2004.

[30] J. M. Mayoral Villa y J. Ramirez, Site response effects on an urban overpass., Journal of Soil Dynamics and Earthquake Engineering, nº ISSN 0267-7261, 2011.

[31] J. M. Mayoral Villa y M. P. Romo, Seismic response of bridges with massive foundations, Journal of Soil Dynamics and Earthquake Engineering, vol. 71, pp. 88-99, 2015.

[32] J. M. Mayoral Villa, S. Tepalcapa, A. Roman, C. S. Mohtar y R. Rivas, Ground Subsidence and its implication on building seismic performance, Journal of Soil Dynamic Earthq Eng, vol. 126, 2019.

[33] J. M. Mayoral Villa y G. Mosqueda, Tunnelling and Underground Space Technology incorporating Trenchless Technology Research, Journal of Soil Dynamics and Earthquake Engineering, 2021.

[34] J. M. Mayoral Villa y G. Mosqueda, Seismic interaction of tunnel-building systems on soft clay, Journal Soil Dynamics and Earthquake Engineering, vol. 139, 2020.

[35] H. B. Seed y I. M. Idriss, Soil moduli and damping factors for dynamic response analysis, vol. 70, nº 10, 1970.

[36] M. P. Romo, Clay behavior, soil response and soil structure interaction studies in Mexico City, de Proceedings of the third international conference on recent advances in geotechnical earthquake engineering and soil dynamics, San Luis Missouri, USA, 1995.

[37] H. B. Seed, I. M. Idriss , J. Sun , A. Jaime y J. Lysmer, Relationships between soil conditions and earthquake ground motions, Journal Earthq Spectra, vol. 4, nº 2, pp. 687-730, 1988.

[38] J. Lysmer, Analytical Procedures in soil dynamics, University of California, vol. 29, nº ReportNo.EERC78, 1978.

[39] N. Abrahamson, State of the practice of seismic hazard evaluation, de International Conference on Geotechnical & Geological Engineering, Australia, 2000.

[40] I. C. Group, FLAC3D, fast Lagrangian analysis of continua in 3 dimensions.

[41] P. B. Schnabel, J. Lysmer y H. B. Seed, SHAKE: a computer program for earthquake response analysis of horizontally layered sites, College of Engineering, CA., 1972.

[42] J. M. Mayoral Villa, Seismic response of bridges with massive foundations, Soil Dynamics and Earthquake Engineering, vol. 71, pp. 88-99, 2015.

[43] J. M. Mayoral Villa, K. W. Franke y T. Hutchinson, The September 19, 2017 Mw 7.1 Puebla-Mexico city earthquake: Important findings from the field – Overview of Special Edition, Journal Soil Dynamics and Earthquake Engineering, vol. 123, pp. 520-524, 2019.

[44] J. M. Mayoral Villa, D. Asimaki, S. Tepalcapa, S. Wood, A. Roman, T. Hutchinson, K. Franke y G. Montalva, Site effects in Mexico City basin: Past and present, Journal, Soil Dynamics and Earthquake Engineering, vol. 121, pp. 369-382, 2019. O.C. Zienkiewicz, R.C. Taylor, *The finite element method, Vol. I, 4th Edition*. McGraw Hill, 1989.